Supporting Information

Red-Emitting $Cs_2NaScCl_6$:Sm Flexible Films for High-Resolution X-Ray Imaging

Yuxia Li[a,c], Qi Luo[a,c], Xin Huang[b,c], Hao Lu[c,d], Yazhou Yuan[a,c], Xieming Xu[b,c], Shuaihua Wang[b,c], and Shaofan Wu*[b,c]*

[a]College of Chemistry and Materials Science, Fujian Normal University, Fuzhou, 350117, China

[b]Fujian Science & Technology Innovation, Laboratory for Optoelectronic Information of China, Fuzhou, 350108, P. R. China

[c]Key Laboratory of Optoelectronic Materials Chemistry and Physics, Fujian Institute of Research on the Structure of Matter, Chinese Academy of Sciences, Fuzhou, 350002, P. R. China.

[d]University of Chinese Academy of Sciences, Beijing, 100049, P. R. China

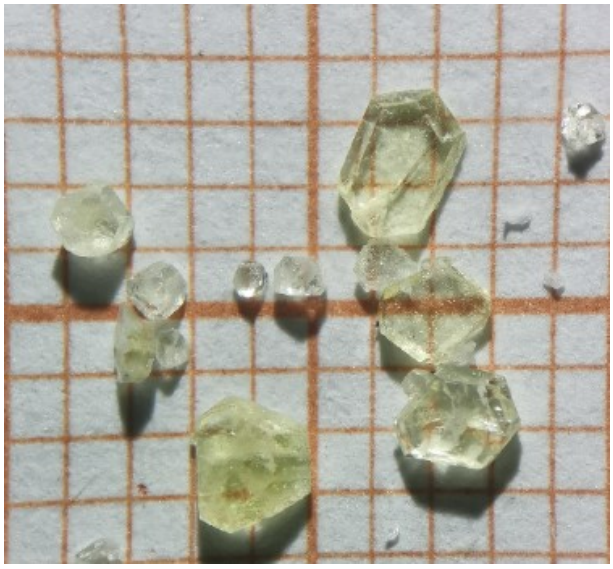

Figure S1. Physical diagram of $Cs_2NaScCl_6$.

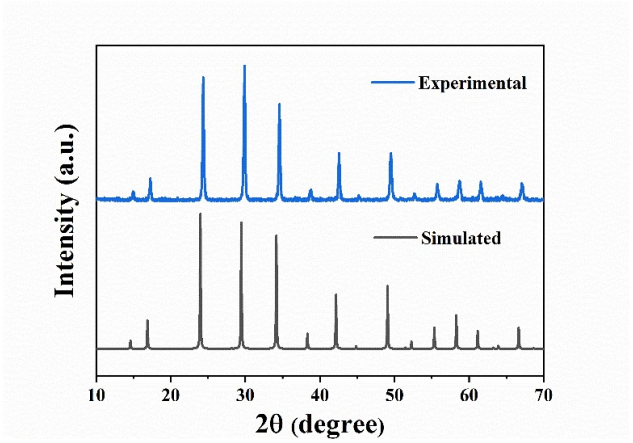

Figure S2. PXRD of $Cs_2NaScCl_6$ compared to the simulated pattern based on SCXRD measurements. It shows that the synthesized material is pure phase, and verifies the accuracy of single crystal data.

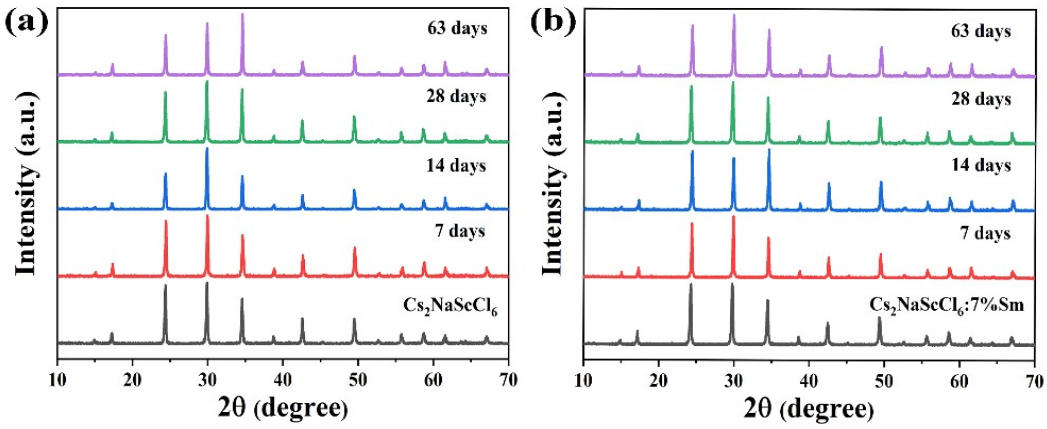

Figure S3. PXRD patterns of $Cs_2NaScCl_6$ and $Cs_2NaScCl_6$:7%Sm crystal powder

exposed to ambient air.

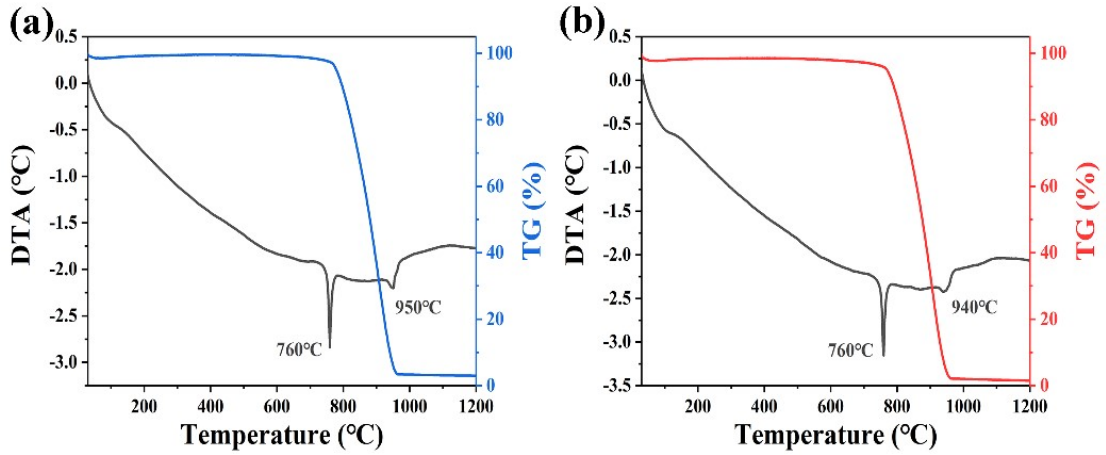

Figure S4. TG and DTA curves of $Cs_2NaScCl_6$ (left), $Cs_2NaScCl_6$:7%Sm (right).

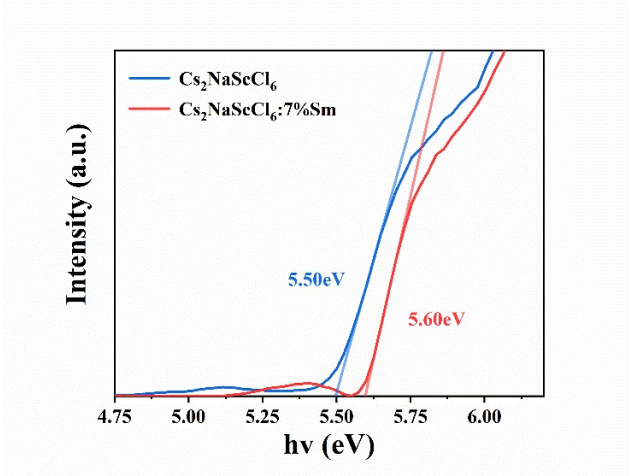

Figure S5. The band gap fitting diagram of $Cs_2NaScCl_6$ and $Cs_2NaScCl_6$:7%Sm.

Attenuation efficiency T is defined as:

$$T = 1 - e^{-\mu_L x}$$

In this equation, μ_L is the linear attenuation coefficient which can be obtained by $\rho_{\mu m}$, x is the effective retarding thickness, ρ is the density of materials and μ_m is the mass attenuation coefficient. The value of μ_m was easily obtained from the photon cross sections database XCOM.

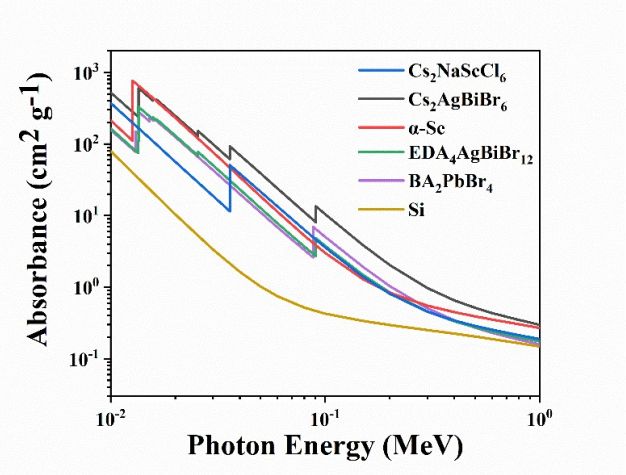

Figure S6. X-ray absorption coefficient spectra of $Cs_2NaScCl_6$ and other scintillating materials.

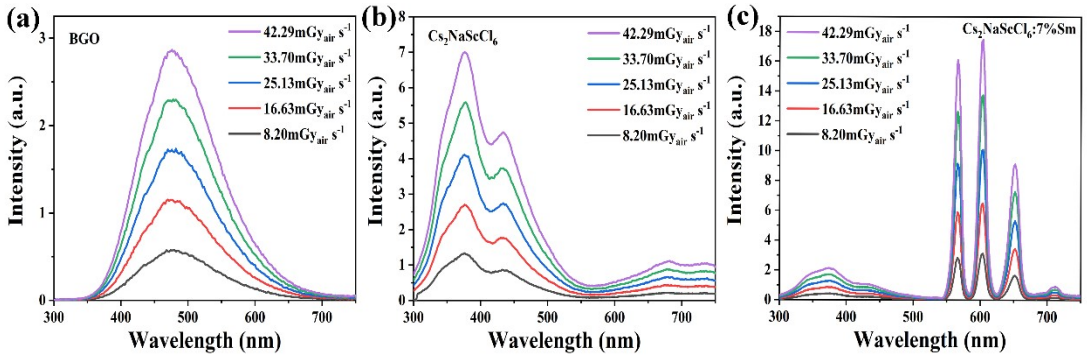

Figure S7. XEL diagram of BGO, $Cs_2NaScCl_6$, and $Cs_2NaScCl_6$:7%Sm at 50kV with different tube currents.

The light yield of $Cs_2NaScCl_6$:7%Sm was calculated with BGO's optical yield of 100.0% as the standard. We measured the response amplitude (R) of the BGO and $Cs_2NaScCl_6$:7%Sm using photo-multiplier tubes (PMT R928). LY is obtained from the following equation:

$$\frac{LY_{sample}}{LY_{BGO}} = \frac{R_{sample}}{R_{BGO}} \times \frac{\int I_{BGO} S(\lambda) d\lambda / \int I_{BGO} d\lambda}{\int I_{sample} S(\lambda) d\lambda / \int I_{sample} d\lambda}$$

where I(λ) is the XEL spectrum and S(λ) in Figure S8 is the detection efficiency of the PMT.

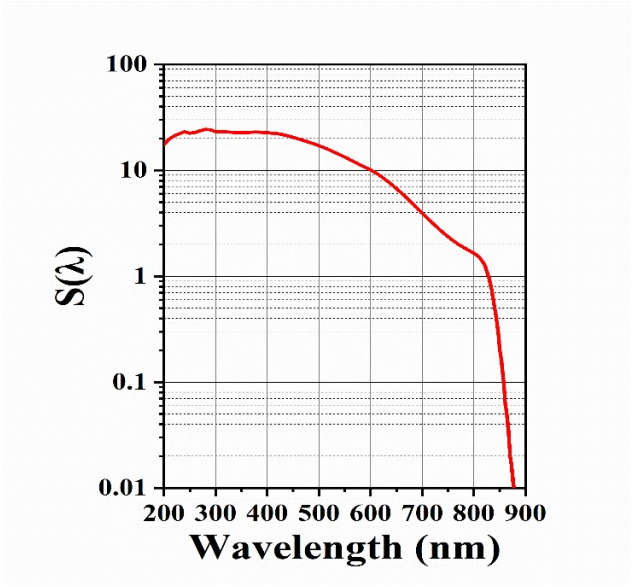

Figure S8. The detection efficiency of PMT.

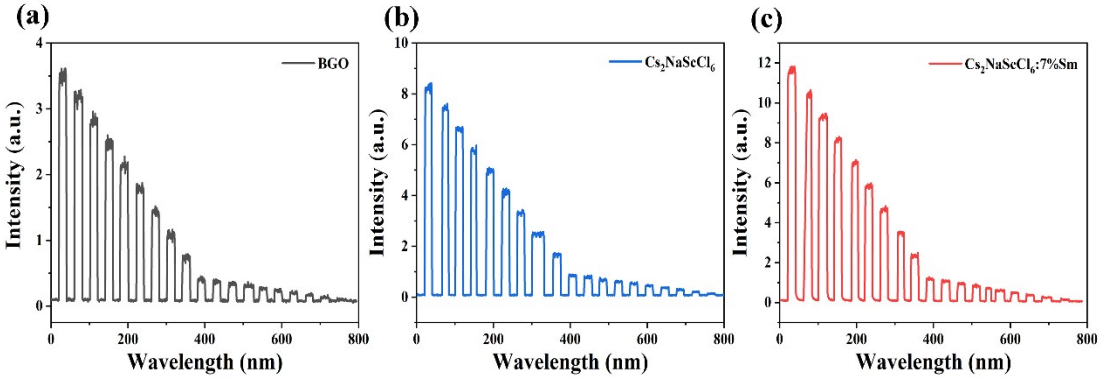

Figure S9. Detection limit test diagram of BGO, $Cs_2NaScCl_6$, and $Cs_2NaScCl_6$:7%Sm at different tube currents at 50 kV.

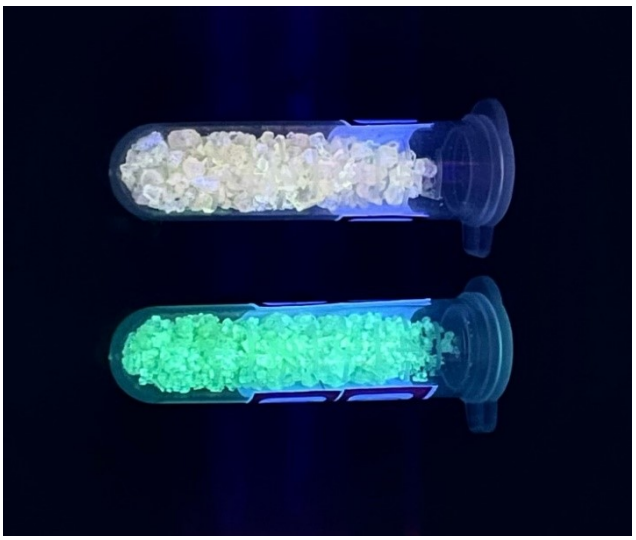

Figure S10. Physical images of $Cs_2NaScCl_6$:7%Sm and $Cs_2NaScCl_6$:10%Tb under 254

nm lamp irradiation in a UV dark box.

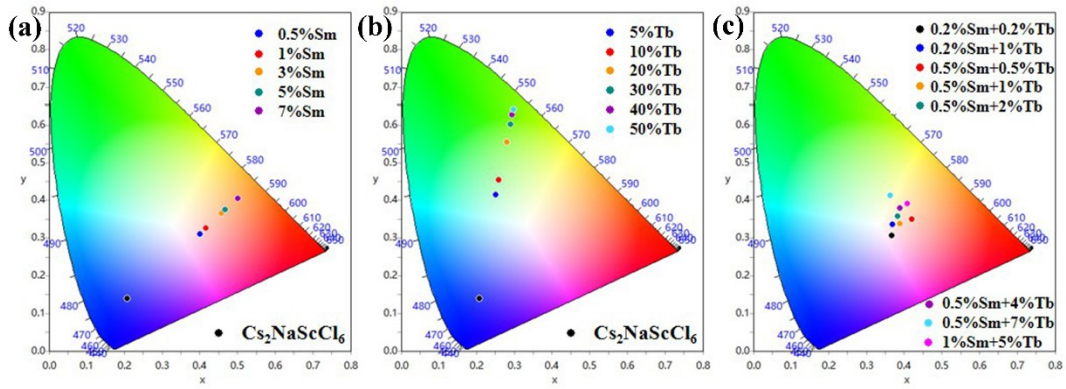

Figure S11. CIE chromaticity diagrams corresponding to X-ray luminescence for $Cs_2NaScCl_6$, $Cs_2NaScCl_6$:xSm, $Cs_2NaScCl_6$:yTb, and $Cs_2NaScCl_6$:xSm,yTb sample powders.

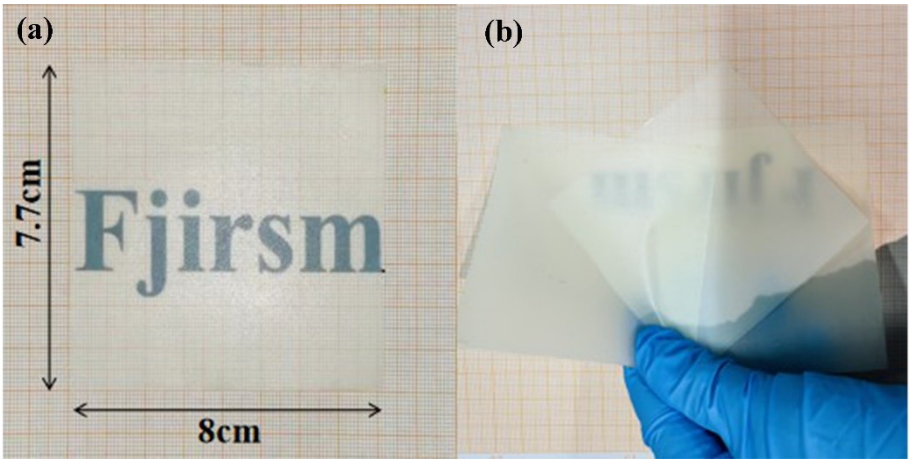

Figure S12. Photographs of $Cs_2NaScCl_6$:7%Sm and other flexible scintillation films.

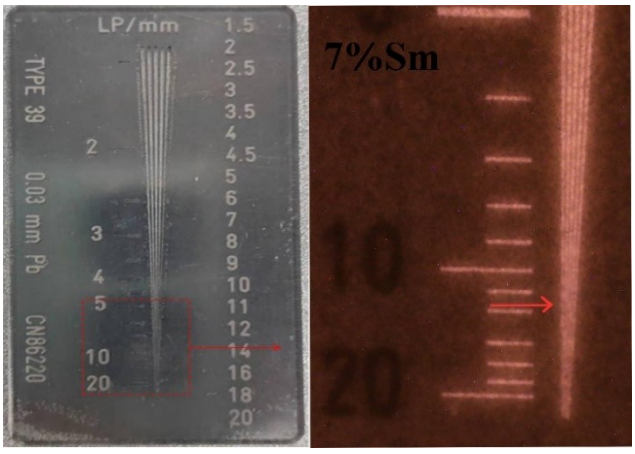

Figure S13. Physical and X-imaging of wire-pair card by $Cs_2NaScCl_6$:7%Sm scintillating film under 8.154 mGyair s^{-1} X-ray irradiation.

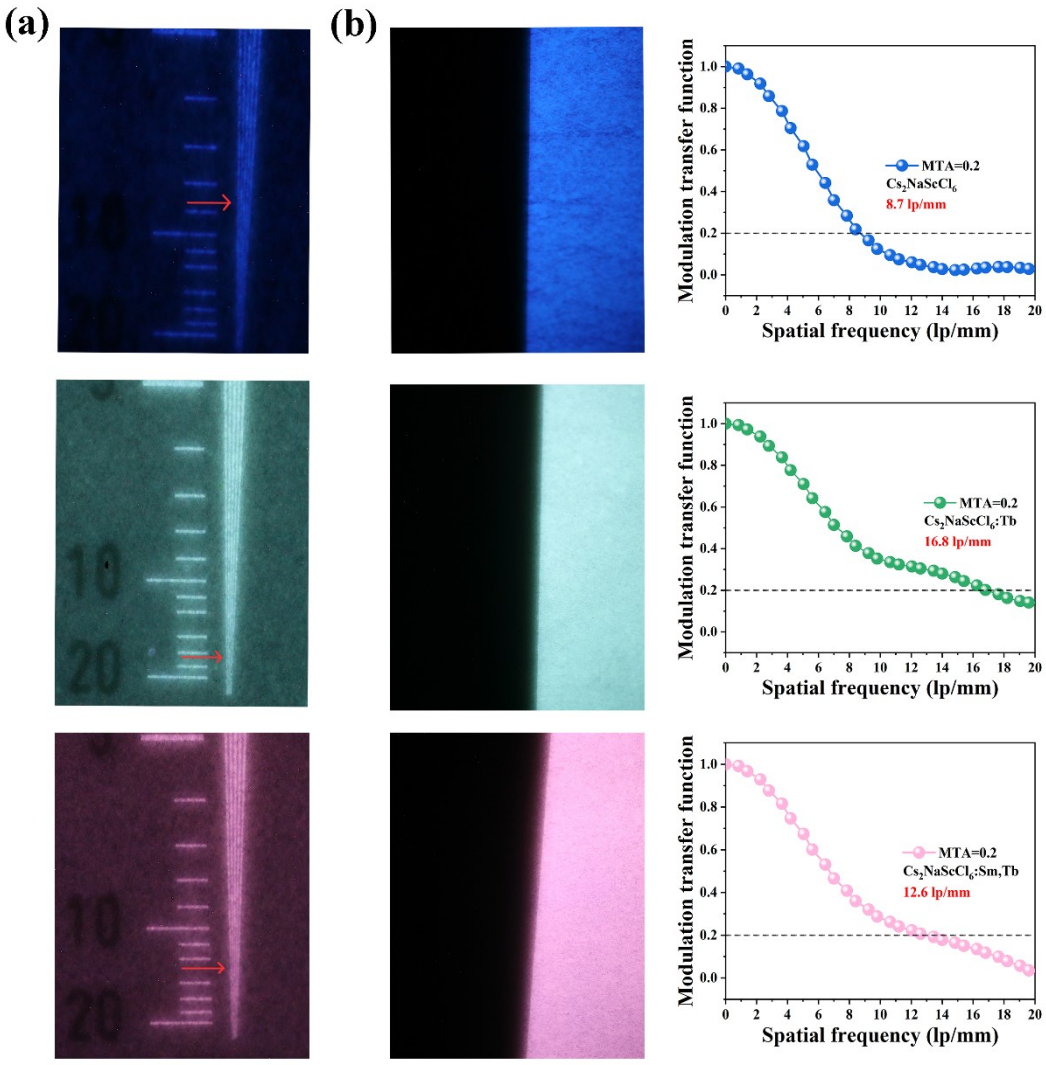

Figure S14. X-ray imaging of $Cs_2NaScCl_6$, $Cs_2NaScCl_6$:10%Tb and $Cs_2NaScCl_6$:0.2%Sm,1%Tb scintillation film pairs of 20 line pairs of standard line pairs and corresponding MTF curves.